Pyrazolate-Based Oligonuclear Copper and Silver Complexes with N/S Coordination Spheres☆

Franc Meyer*, Albrecht Jacobi, and Laszlo Zsolnai

Anorganisch-Chemisches Institut der Universität Heidelberg,
Im Neuenheimer Feld 270, D-69120 Heidelberg, Germany
Fax: (internat.) +49(0)6221/545707
E-mail: Franc@sun0.urz.uni-heidelberg.de

Received February 24, 1997

Keywords: Pyrazolate complexes / Bridging ligands / Copper / Silver / N,S-Donor Ligands

A series of pyrazole-based potential ligands bearing thioether substituents in 3- and 5-positions of the heterocycle was synthesized [3,5-bis($RSCH_2$)-pyzH; R = Ph (**1aH**), $PhCH_2$ (**1bH**), *i*Pr (**1cH**), *t*Bu (**1dH**)]. These ligands afford oligonuclear Cu^I and Ag^I coordination compounds $[LCu]_x$ (**2a**–**c**, L = **1a**–**c**) and $[LAg]_x$ (**3a**–**d**, L = **1a**–**d**), respectively. The single crystal X-ray analysis of **3c** shows the presence of trimeric planar arrays of N,N'-bridging pyrazolates and linear coordinated silver ions, with each two of the trinuclear moieties being linked by two unsupported short intermolecular Ag···Ag contacts [3.041(1) Å]. Molecular-weight determinations for **2a** (THF) and **3c** (toluene) indicate that hexanuclear entities are preserved in solution. Starting from **1bH** the Cu^{II} complex $[(\mathbf{1b})_2Cu_2](BF_4)_2$ (**4**) was synthesized. According to an X-ray crystal structure analysis it consists of dinuclear molecules with two bridging pyrazolates, distorted square planar N_2S_2 coordination spheres for Cu^{II} and an axially bridging tetrafluoroborate. Magnetic susceptibility data reveal an antiferromagnetic exchange (J = -206 cm^{-1}) that is among the highest found for doubly pyrazolate bridged dicopper(II) complexes, which is rationalized on the basis of the rather symmetric dinuclear core of **4**. The irreversibility of the electrochemical reduction and oxidation processes for the Cu^{II} and Cu^I compounds, respectively, is explained by the inability of the respective coordination framework to adapt to different geometric preferences.

Introduction

Stimulated by the occurrence of N/S coordinated copper ions in a variety of proteins[1], numerous ligands with N and S donor atoms have been synthesized and investigated in order to model the properties of these metallobiosites[2–4]. Biological systems like the mononuclear "blue" type-1 copper sites and the dinuclear Cu_A center in cytochrome C oxidase are involved in electron transfer processes during enzyme turnover[1,5]. The latter were recently shown to consist of a bis(cysteinato)-bridged delocalized mixed-valence Cu(1.5)Cu(1.5) entity[6], and consequently much effort has been devoted to the study of dinuclear copper model complexes with bridging thiolates and terminal N donor atoms[7,8]. With regard to a general study of the properties of dimeric copper units in a mixed N/S environment it appeared of interest to also investigate inverse systems, i.e. those incorporating bridging nitrogen moieties and terminal thioether coordination. In this work we describe the synthesis and characterization of dinuclear Cu^{II} as well as oligonuclear Cu^I and Ag^I complexes of a series of N,N'-bridging pyrazolates with chelating thioether ligation. The ability of the diazole unit of pyrazolates to bridge two metal centers is well documented[9]. However, relatively few studies of pyrazolate-based ligands bearing additional side arms in the 3- and 5-positions of the heterocycle have been reported, and most of those systems possess N-donors in the substituents[10–14]. On the other hand various mononuclear complexes of chelating ligands containing both azole and thioether moieties have been designed as model complexes for type 1 copper proteins[3,4a,15]. In the present study multinuclear copper complexes of mixed N/S donor systems based on bridging diazole heterocycles are investigated. Likewise related silver(I) complexes are studied for structural comparison with the corresponding copper(I) species.

A further motivation for this work arises from the versatile coordination properties of pyrazole and its derivatives with respect to the formation of multimetallic transition-metal complexes[16]. For example Cu^I-pyrazolates of general formula $[Cu(3,5\text{-}R_2pz)]_x$ were obtained as trinuclear[17,18], tetranuclear[19], or polymeric[20] species depending on the reaction conditions and on the nature of the R substituents (generally non-coordinating substituents like R = H, Me, Ph, COOMe). The nuclearity of such complexes is expected to be markedly influenced by the presence of additional chelating thioether donor sites in the side arms of the pyrazolate ligands employed in the present study.

Results and Discussion

The dinucleating N_2S_2 ligands with a pyrazole backbone were prepared as outlined in Scheme 1. 3,5-Bis(chloromethyl)pyrazole is accessible in four steps from 3,5-dimethylpyrazol following a method described by Bosnich et al.[10] Treatment with three equivalents of the respective thiolate yields quadridentate potential ligands **1aH**–**dH** in good yields, which were purified by column chromatography.

0009–2940/97/1010–1441 $ 17.50+.50/0

Their spectroscopic and analytical data are summarized in Tables 1−4.

Scheme 1. Synthesis of the ligands

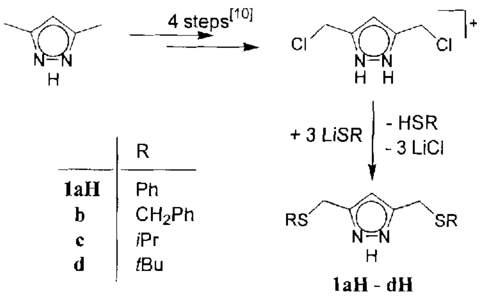

	R
1aH	Ph
b	CH₂Ph
c	*i*Pr
d	*t*Bu

Table 1. ^{1}H-/^{13}C-NMR data of the free ligands **1aH−dH** and the complexes **2a−c**, **3a−d**[a]

	$C^{3/5}$	C^4H	CH_2	R
1aH[b]	144.9	6.09 / 104.4	4.08 / 30.0	7.20–7.28 (m, 10 H, Ph) / 126.3, 128.7, 129.5, 135.5
1bH[b]	145.7	6.12 / 104.6	3.68 / 26.8[d]	3.61 (s, 2 H, CH_2) / 35.9; 7.25–7.33 (m, 10 H, Ph) / 127.1, 128.5, 129.0
1cH[b]	146.2	6.17 / 104.0	3.75 / 26.5	1.26 (d, $^{3}J_{HH}$ = 6.7 Hz, 6 H, CH_3) / 23.0; 2.87 (sept, $^{3}J_{HH}$ = 6.7 Hz, 1 H, CH) / 34.9
1dH[b]	not found	6.16 / 103.7	3.77 / 24.8	1.32 (s, 18 H, CH_3) / 30.7; 42.9
2a[b]	149.5	6.09 / 104.2	4.19 / 31.6	7.16–7.27 (m, 10 H, Ph) / 126.3, 128.8, 129.4, 135.8
2b[c]	149.6	5.94 / 104.6	3.68 / 28.4[d]	3.47 (s, 2 H, CH_2) / 35.6; 6.95–7.20 (m, 10 H, Ph) / 126.7, 128.2, 128.9, 138.0
2c[c]	150.0	6.12 / 104.3	3.92 / 28.5	1.12 (d, $^{3}J_{HH}$ = 6.7 Hz, 6 H, CH_3) / 23.2; 2.81 (sept, $^{3}J_{HH}$ = 6.7 Hz, 1 H, CH) / 34.8
3a[b]	149.5	6.13 / 103.5	4.04 / 31.8	7.13–7.21 (m, 10 H, Ph) / 126.3, 128.8, 129.3, 135.9
3b[c]	149.1	6.09 / 103.7	3.66 / 28.7[d]	3.63 (s, 2 H, CH_2) / 35.9; 7.01–7.31 (m, 10 H, Ph) / 126.7, 128.2, 129.0, 138.2
3c[b]	149.9	6.17 / 102.8	3.85 / 28.2	1.27 (d, $^{3}J_{HH}$ = 6.7 Hz, 6 H, CH_3) / 23.1; 2.89 (sept, $^{3}J_{HH}$ = 6.7 Hz, 1 H, CH) / 34.6
3d[b]	150.9	6.22 / 102.2	3.87 / 26.8	1.34 (s, 18 H, CH_3) / 31.1; 43.5

[a] δ in ppm. − [b] Solvent $CDCl_3$. − [c] Solvent C_6D_6. − [d] The assignment of the two different CH_2 groups is arbitrary.

Table 2. Analytical data for all new compouds

	C calcd. (found)	H calcd. (found)	N calcd. (found)
1aH	65.35 (65.36)	5.16 (5.22)	8.97 (8.90)
1bH	67.02 (66.71)	5.92 (6.14)	8.23 (8.09)
1cH	54.05 (53.88)	8.25 (8.36)	11.46 (11.34)
1dH	57.30 (57.93)	8.88 (9.04)	10.28 (9.96)
2a	54.45 (53.60)	4.03 (4.14)	7.47 (7.24)
2b	56.62 (56.69)	4.75 (4.79)	6.95 (6.97)
2c	43.04 (43.29)	6.24 (6.31)	9.13 (9.18)
3a[a]	45.52 (45.51)	3.49 (3.58)	6.07 (6.18)
3b	51.01 (50.66)	4.28 (4.34)	6.26 (6.14)
3c	37.61 (37.54)	5.45 (5.49)	7.97 (7.91)
3d	41.16 (41.98)	6.11 (5.79)	7.38 (7.48)
4	46.59 (46.73)	3.91 (4.09)	5.72 (5.77)

[a] Calculated for **3a** · CH_2Cl_2.

Table 3. Selected IR absorptions of all new compounds

	Selected IR absorptions [cm^{-1}]
1aH	1583 (s), 1480 (s), 1439 (s), 1315 (m), 1234 (m), 1023 (s), 739 (s), 690 (s)
1bH	1600 (w), 1572 (m), 1494 (s), 1453 (s), 1417 (m), 1315 (m), 1231 (m), 1069 (m), 1027 (m), 701 (s)
1cH	1572 (m), 1462 (m), 1235 (m), 1154 (m), 1051 (m), 1002 (m)
1dH	1588 (m), 1472 (m), 1459 (m), 1314 (m), 1156 (s), 1022 (m), 851 (s,br)
2a	1582 (m), 1517 (m), 1476 (s), 1438 (m), 1415 (m), 1231 (m), 1025 (m), 735 (s), 690 (s)
2b	1600 (w), 1516 (m), 1493 (m), 1452 (m), 1415 (m), 1358 (m), 1231 (m), 1069 (m), 698 (s)
2c	1517 (m), 1452 (m), 1364 (m), 1233 (m), 1154 (m), 1051 (m), 802 (m), 792 (m), 737 (m)
3a	1583 (s), 1512 (m), 1480 (s), 1438 (s), 1414 (w), 1233 (m), 1025 (m), 735 (s), 690 (s)
3b	1600 (w), 1514 (m), 1491 (m), 1448 (m), 1417 (m), 1343 (m), 1227 (m), 1128 (m), 696 (s)
3c	1512 (m), 1462 (m), 1447 (m), 1381 (m), 1364 (m), 1233 (m), 1154 (m), 1053 (m), 791 (m)
3d	1514 (m), 1468 (m), 1459 (m), 1364 (m), 1160 (m), 792 (m,br)
4	1600 (w), 1515 (m), 1495 (m), 1454 (m), 1403 (m), 1234 (m), 1047 (s,br), 770 (m), 701 (s)

Synthesis and Characterization of Cu^{I} and Ag^{I} Complexes

Deprotonation of **1aH−dH** by means of BuLi and subsequent addition of one equivalent of CuCl or $AgBF_4$ affords white coordination compounds $[LCu]_x$ (**2a−c**, L = **1a−c**) and $[LAg]_x$ (**3a−d**, L = **1a−d**), respectively, which are readily soluble in petroleum ether, chlorinated or aromatic solvents, but are insoluble in more polar solvents like acetone or methanol. Thus they can alternatively be prepared by adding stoichiometric amounts of CuCl or $AgBF_4$ to an acetone solution of **1aH−dH** and NEt_3, causing the gradual precipitation of complexes **2a−c** and **3a−d**, respectively. Analytical data for all complexes confirm a ligand-to-metal stoichiometry of 1:1, Table 2. A significant shift of the IR absorption for the highest ring nuclear vibration, ω[21] (attributed to $\nu_{C=N}$; 1570−1590 cm^{-1} in **1a−d** vs. 1510−1520 cm^{-1} in **2a−c**, **3a−d**, Table 3) is indicative of the *N*-coordination of the pyrazolate. However, chemical shifts of the ^{1}H- and ^{13}C-NMR signals for **2a−c** and **3a−d** (Table 1) do not differ considerably from the corresponding ones of the free ligands.

Table 4. Major mass-spectrometric fragments

	Major mass-spectrometric fragments
1aH[a]	313 (97) [M^+ + 1], 203 (100) [M^+ − SPh]
1bH[a]	341 (100) [M^+ + 1]
1cH[a]	245 (100) [M^+ + 1]
1dH[a]	273 (100) [M^+ + 1]
2a[b]	2247.0 (25) [$(\mathbf{1a})_6Cu_6^+$], 1499.9 (67) [$(\mathbf{1a})_4Cu_4^+$], 1123.9 (100) [$(\mathbf{1a})_3Cu_3^+$]
2b[b]	2483.0 (9) [$(\mathbf{1b})_6Cu_7^+$], 2420.0 (9) [$(\mathbf{1b})_6Cu_6^+$], 2077.8 (27) [$(\mathbf{1b})_5Cu_6^+$], 1612.7 (85) [$(\mathbf{1b})_4Cu_4^+$], 1208.6 (100) [$(\mathbf{1b})_3Cu_3^+$], 806.4 (40) [$(\mathbf{1b})_2Cu_2^+$]
2c[b]	1903.3 (7) [$(\mathbf{1c})_6Cu_7^+$], 1840.5 (8) [$(\mathbf{1c})_6Cu_6^+$], 1597.1 (14) [$(\mathbf{1c})_5Cu_6^+$], 1226.1 (100) [$(\mathbf{1c})_4Cu_4^+$], 920.1 (49) [$(\mathbf{1c})_3Cu_3^+$]
3c[b]	2212.9 (28) [$(\mathbf{1c})_6Ag_7^+$], 2060.9 (32) [$\{(\mathbf{1c})_6Ag_6\text{-}i\mathrm{Pr}\}^+$], 1862.4 (100) [$(\mathbf{1c})_5Ag_6^+$], 1711.8 (47) [$\{(\mathbf{1c})_5Ag_5\text{-}i\mathrm{Pr}\}^+$], 1512.9 (74) [$(\mathbf{1c})_4Ag_5^+$], 1054.0 (49) [$(\mathbf{1c})_3Ag_3^+$]
4[c]	893 (64) [$(\mathbf{1b})_2Cu_2(BF_4)^+$], 806 (58) [$(\mathbf{1b})_2Cu_2^+$], 467 (100) [$(\mathbf{1a})Cu_2^+$]

[a] EI mass spectra. − [b] FD mass spectra. − [c] FAB mass spectrum.

FD mass spectra of the complexes **2a−c** and **3c** show peaks at values *m*/*z* corresponding to $[LCu]_x$ and $[LAg]_x$

($x \geq 2$) with the expected isotopic distribution pattern in each case, thus suggesting the presence of oligonuclear species in these systems (Table 4). The spectrum of **2a** is depicted in Figure 1.

Figure 1. FD mass spectrum of **2a**; the inset shows the experimental (upper) and theoretical (lower) isotopic distribution for the trimer [**1a**Cu]$_3$

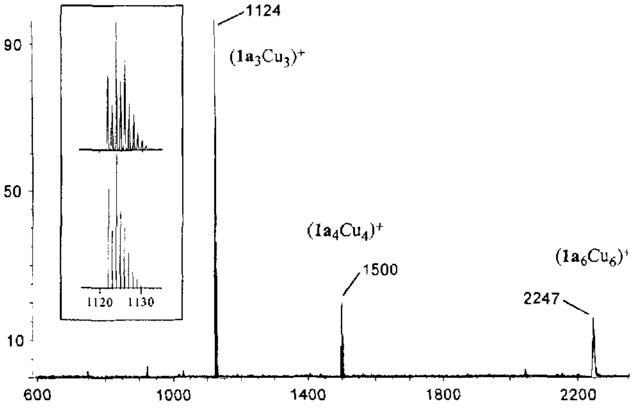

It displays a dominant peak for the trimer [**1a**Cu]$_3$ (m/z = 1124) and signals at values m/z corresponding to the tetrameric (m/z = 1500) and hexameric (m/z = 2247) species. The absence of a signal for the pentamer as well as the observation that the intensity of the signal for the hexamer decreases at higher scan numbers during the FD-MS experiment might suggest the latter to be a cluster of two trimers rather than a discrete hexameric complex. Unfortunately our attempts to grow single crystals of any of the Cu^I compounds were unsuccessful, in all cases only providing cotton-like material. However, colorless needles of the silver complex **3c** suitable for X-ray crystal structure analysis could be obtained by slow cooling of a 1,2-dichloropropane/acetone solution to −30°C.

Description of the Structure of 3c

The molecular structure of **3c**, which crystallizes in the monoclinic space group $P2_1/n$, is depicted in Figure 2. It shows the presence of a trinuclear cyclic array of three nearly linearly coordinated silver ions [N−Ag−N in the range 170.7(2)° to 174.9(2)°] and three N,N'-bridging pyrazolates, similar to the triangular framework found for some related simple pyrazolate complexes of the coinage metal ions[17,18,22]. The Ag_3N_6 ring skeleton in **3c** is planar within 0.09 Å, showing relatively short Ag−N bond lengths [2.074(6)−2.120(6) Å] and nonbonding intramolecular Ag···Ag distances ranging from 3.453 to 3.700 Å. The thioether side arms are non-coordinating, the shortest distances Ag···S amounting to 3.094 Å (Ag1−S1) and 3.111 Å (Ag2−S2), clearly longer than the maximum bond length generally accepted for Ag^I−S bonds (3.01 Å)[23]. Comparable atom distances between Ag^I and S observed in some thiophene[23] and isothiazole[24] complexes were shown to be of negligible bonding character and to consist of no more than a dipole−cation attraction. It should be noted that long Cu···S(thioether) contacts were discussed by Schilstra et al.[25] on the basis of Cu···S−C angles, i.e. the positions of the lone electron pairs on the S atoms. While Cu−S−C angles larger than 90°C are observed for complex structures in which the thioether side arm is coordinating (compare: Cu−S−C angles in the range 93.8−118.5° are observed for **4**, see below), smaller Cu···S−C angles were suggested to indicate that the lone pairs on the S atoms do not point toward the metal ion[25]. In the present compound **3c** the Cu···S−C angles are found in the range 84.2−93.9°, i.e. although not allowing a decisive conclusion they are relatively small and thus render any bonding interaction unlikely.

Figure 2. View of the molecular structure of **3c** (top; in the interests of clarity all hydrogen atoms have been omitted) and the trimer-trimer interactions (bottom)

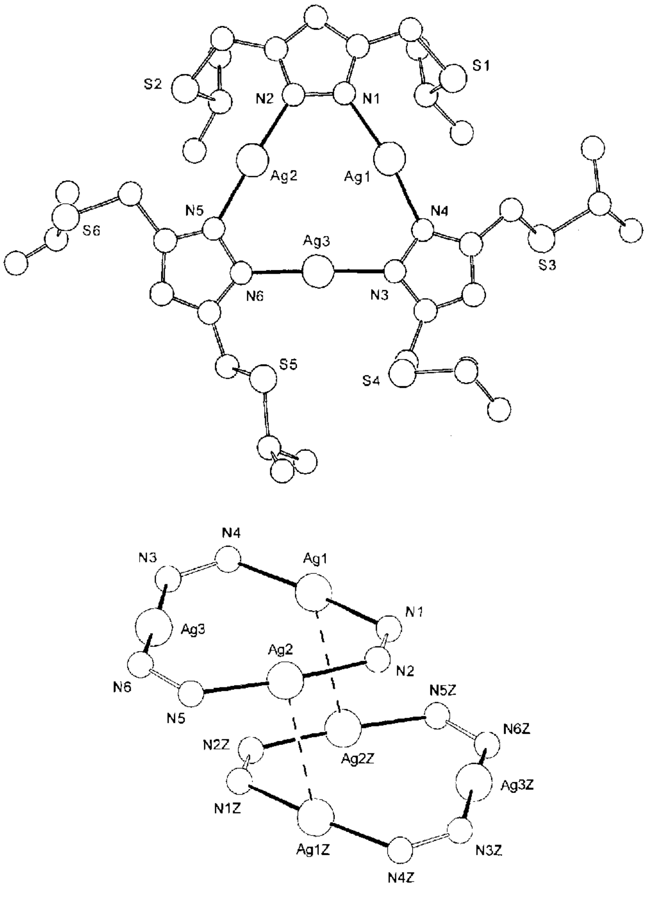

Table 5. Selected atom distances [Å] and angles [°] for **3c** (estimated standard deviations in parentheses)

Ag1–N1	2.120(6)	N1–Ag1–N4	170.7(2)
Ag1–N4	2.105(6)	N2–Ag2–N5	174.9(2)
Ag2–N2	2.083(5)	N3–Ag3–N6	173.3(2)
Ag2–N5	2.085(5)	N1–Ag1–Ag2Z	78.0(2)
Ag3–N3	2.074(6)	N4–Ag1–Ag2Z	105.1(2)
Ag3–N6	2.086(6)	N2–Ag2–Ag1Z	81.6(2)
N1–N2	1.372(7)	N5–Ag2–Ag1Z	103.0(2)
N3–N4	1.374(7)	N1–N2–Ag2	124.3(4)
N5–N6	1.366(8)	N2–N1–Ag1	122.9(4)
Ag1–Ag2Z	3.041(1)	N3–N4–Ag1	119.7(4)
Ag1···S1	3.094	N4–N3–Ag3	123.8(4)
Ag2···S2	3.111	N5–N6–Ag3	121.3(4)
		N6–N5–Ag2	117.9(4)

A striking feature of the structure of **3c** is the arrangement of each two trimers in pairs about crystallographic inversion centers in the crystal lattice, resulting in two short unsupported interdimer Ag···Ag separations [3.041(1) Å] as depicted in the lower part of Figure 2. This distance being significantly smaller than the sum of the van der Waals radii (3.40 Å)[26], but longer than the atom distances in silver metal (2.889 Å), resembles the bond lengths found for some other non-bridged Ag···Ag systems (typically in the range 2.8–3.3 Å)[27]. The remaining third Ag atom (Ag3 and Ag3Z, respectively) is located above a pyrazolate ring of the inversion-related trimer unit and the entire assembly is wrapped in the hydrophobic thioether side arms. The central structure of **3c** is thus very similar to those reported recently for two related Cu^I complexes consisting of triangular molecules linked by weak Cu···Cu interactions[18], while the only other pyrazolate-based trinuclear Ag^I complexes characterized structurally either show significantly longer Ag···Ag intertrimer contacts [3.431(4) Å][28] or a much more puckered framework with non-interacting individual trimers[22].

The mass-spectrometric findings discussed above as well as the very similar appearance and solubility of the Cu^I and the Ag^I complexes studied in this work suggest the existence of similar molecular structures in all compounds. Molecular weight determinations in solution (vapor-phase osmometry) were carried out for **2a** (thf) and **3c** (toluene), yielding molecular masses of 2200 g · mol^{-1} and 2050 g · mol^{-1}, respectively, in accord with the presence of hexameric complexes $[\mathbf{1a}Cu]_6$ (M = 2250 g · mol^{-1}) and $[\mathbf{1c}Ag]_6$ (M = 2106 g · mol^{-1}) (it should be noted, however, that the accuracy of the molecular weight determination of **2a** suffers from the gradual decomposition of this Cu^I complex in solution, see below). It thus appears that the dimeric assembly of trinuclear cyclic arrays resulting solely from intermolecular Ag···Ag interactions between closed-shell d^{10} systems as observed in the solid state in the case of **3c** remains intact upon dissolution, and it furthermore suggests that this is also the case in the homologous Cu^I compounds. However, these species in solution either have to be of high symmetry or highly fluxional, as the ^1H- and ^{13}C-NMR spectra exhibit only one set of resonances, even if a sample of **2d** in CD_2Cl_2 is cooled to −90°C.

Complexes **2a–c** and **3a–d** are stable in the solid state over prolonged periods. However, in solution the Cu^I compounds slowly decompose to unidentified green Cu^{II} species even under an inert atmosphere, the phenyl-substituted **2a** being slightly more stable than **2b**, **c**. Cyclic voltammograms of CH_2Cl_2 solutions of **2a**, **b** display irreversible oxidation processes at high potentials $E_p^{ox} = +0.90$ V (**2a**) and +0.86 V (**2b**) vs. SCE, which are followed by corresponding irreversibel reduction waves at +0.24 V (**2a**) and +0.12 V (**2b**). Obviously the oxidation of Cu^I in these complexes is accompanied with a fast chemical transformation generating a coordination framework more suitable for the stabilization of Cu^{II}. In order to gain further insight into the structures of possible Cu^{II} complexes of the present class of ligands, a representative compound was synthesized and studied independently.

Synthesis and General Characterization of 4

Treatment of **1b** with one equivalent of $[Cu(H_2O)_6](BF_4)_2$ affords the dark-brown Cu^{II} complex **4**, whose elemental analysis is in accord with a ligand/metal/BF_4 stoichiometry of 1:1:1. Its FAB-MS spectrum (Table 4) with *m/z* = 893 corresponding to $\{[\mathbf{1b}Cu]_2(BF_4)\}^+$ as the signal of highest mass supports the presence of dimeric species $[\mathbf{1b}Cu]_2(BF_4)_2$ as confirmed by an X-ray crystal structure (see below). The solution UV/Vis spectrum of **4** displays an absorption at 480 nm which is obscured by a more intense broad band peaking at 330 nm [ε = 9800; assigned to a $S(\sigma) \rightarrow Cu^{II}$ LMCT transition[29]] suggesting coordination of the thioether-S to the metal centers. Cyclic voltammetry (CH_2Cl_2, 200 mV/s) yields an irreversible reduction at $E_p^{red} = +0.15$ V (a two electron process as shown by coulometry) followed by a corresponding oxidation wave at +0.77 V.

X-band EPR spectra of **4** were recorded for a powdered sample and in CH_2Cl_2 solution. At room temperature only a broad signal is observed in both cases. Cooling to 110 K causes the intensity of the spectra to decrease significantly, due to depopulation of the triplet state, however a better resolution is obtained. The powder spectrum is typical for a strongly coupled dinuclear copper and the half-field transition ($\Delta m_s = \pm 2$) is observed at $g = 4.40$.

Description of the Structure of 4

Single crystals suitable for X-ray analysis could be obtained by layering a solution of **4** in acetone with petroleum ether at room temperature. **4** crystallizes in the triclinic space group $P\bar{1}$ with two dimeric molecular moieties and two solvent molecules in the unit cell. Its molecular structure is depicted in Figure 3.

Figure 3. Molecular structure of **4**; in the interests of clarity all hydrogen atoms have been omitted

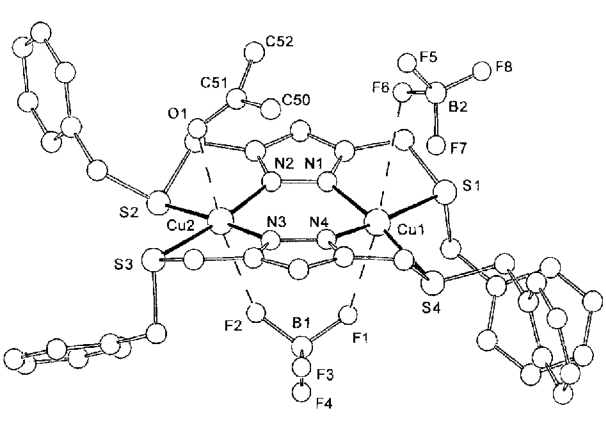

4 contains dinuclear units $[\mathbf{1b}Cu]_2^{2+}$ incorporating two bridging pyrazolates. Each copper center is coordinated by two pyrazolate-N and two thioether-S, resulting in a distorted square planar N_2S_2 coordination sphere. The Cu–S distances [2.345(2)–2.365(2) Å] lie within the normal range

Table 6. Selected atom distances [Å] and angles [°] for **4** (estimated standard deviations in parentheses)

Cu1–N1	1.940(6)	N1–Cu1–N4	97.9(2)
Cu1–N4	1.944(6)	N1–Cu1–S1	85.1(2)
Cu1–S1	2.345(2)	N1–Cu1–S4	172.3(2)
Cu1–S4	2.365(2)	N4–Cu1–S1	171.1(2)
Cu1–F1	2.642(8)	N4–Cu1–S4	80.8(2)
Cu1–F6	2.454(8)	S1–Cu1–S4	97.4(1)
Cu2–N2	1.936(6)	N2–Cu2–N3	99.1(2)
Cu2–N3	1.937(6)	N2–Cu2–S2	83.2(2)
Cu2–S2	2.347(2)	N3–Cu2–S2	176.4(2)
Cu2–S3	2.351(2)	N3–Cu2–S3	84.3(2)
Cu2–F2	2.691(7)	N2–Cu2–S3	174.3(2)
Cu2–O1	2.618(6)	S2–Cu2–S3	93.7(1)
Cu1···Cu2	3.828	N2–N1–Cu1	129.4(4)
N1–N2	1.364(8)	N1–N2–Cu2	129.5(4)
N3–N4	1.362(8)	N3–N4–Cu1	130.1(4)
		N4–N3–Cu2	128.7(4)

usually expected for Cu^{II} thioether bonds[4,15]. Additional weak interactions with two BF_4^- counteranions in the case of Cu1 {Cu1–F1: 2.642(5) Å; Cu1–F6X: 2.451(7) Å [Cu1–F6: 2.999(6) Å]} or one BF_4^- and the oxygen atom of an acetone molecule in the case of Cu2 (Cu2–F2: 2.691 Å; Cu2–O1: 2.618 Å) complete a strongly Jahn-Teller-distorted octahedral coordination geometry. One of the BF_4^- ions thus occupies a bridging position, causing the two basal N_2S_2 planes of the two copper centers to deviate from coplanarity and to tilt towards each other intersecting at 26.8°. It should be noted that only few crystallographic examples of bridging tetrafluoroborate anions have been reported previously[30]. The planes defined by the two pyrazolate rings intersect at 15.3°. The Cu···Cu distance is found to be 3.828 Å. In the dinuclear assembly the observed angles N–Cu–N [N1–Cu1–N4: 97.9(2)°; N2–Cu2–N3: 99.1(2)°] and N–N–Cu [lying in the range 128.7(4)–130.1(4)°] are close to the values considered as so-called optimum angles based on simple considerations on the geometry of doubly pyrazolate bridged complexes[31] and should thus allow a fairly efficient overlap between the copper d_{x2-y2} and the pyrazolate N σ orbitals.

Magnetic Properties of 4

Studies in solution (CD_2Cl_2; Evans method[32]) revealed a subnormal magnetic moment of 1.1 μ_B per copper atom for **4** at room temperature, suggesting the operation of an antiferromagnetic spin exchange within each molecule. Variable-temperature magnetic susceptibility measurements were performed on a dried, powdered sample in the temperature range 97–300 K. The results are displayed in Figure 4.

The shape of the susceptibility plot is typical for an antiferromagnetically coupled dicopper(II,II) compound and the curve was fitted by use of the adapted Bleaney-Bowers equation[33] (Eq. 1) for $S = 1/2$ dimers with a singlet-triplet gap $2J$, where p represents the fraction of uncoupled paramagnetic impurity. All other parameters have their usual meanings.

$$\chi_m = (2\,N\beta^2 g^2)/kT)[3 + \exp(-2J/kT)]^{-1}(1 - p)\;(N\beta^2 g^2)/2\,kT)p \qquad (1)$$

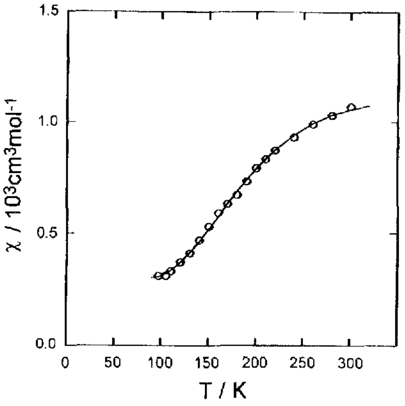

Figure 4. Temperature dependence of the magnetic susceptibility for **4**; the solid line represents the calculated curve ($J = -206$ cm^{-1}, $g = 2.03$, $p = 0.03$)

The solid line results from the best fit of the experimental data that was obtained for the values $J = -206$ cm^{-1}, $g = 2.03$, and $p = 0.03$. It is assumed that the dominant pathway for magnetic exchange is propagated via the bridging pyrazolates, while the bridging tetrafluoroborate should not contribute significantly to the superexchange, even more because it does not link the copper(II) ions in the equatorial plane of the two d_{x2-y2} magnetic orbitals. The observed J value lies in the upper range of the exchange interactions found for related bis(μ-pyrazolato)-bridged complexes, although the number of structurally characterized examples reported in the literature is still limited[11a,b,12,31,34]. A magnetostructural correlation for this type of compounds as investigated by Ajo et al.[35] relates the singlet-triplet energy gap to the angle between the two copper coordination planes and the angle formed by the two pyrazolate rings. Deviation of the latter from coplanarity is predicted to have the most significant effect on the exchange interaction, which was later corroborated by comparison of experimental J values for different representative compounds[11a,b,12]. The largest exchange interaction propagated through double pyrazolate bridges recorded so far amounts to −214 cm^{-1} for the coplanar system $[Cu_2L_2][BPh_4]_2$ {HL = 3,5-bis[(2-diethylamino)ethylaminomethyl]pyrazol}[11a], only slightly higher than the value found in the present complex showing an angle of 15.3° between the planes of the pyrazolate moieties. In recent work Hanot et al.[31] considered another geometrical factor, namely the asymmetry of the $Cu(NN)_2Cu$ framework, in order to account for the differences of the antiferromagnetic coupling constant in several nearly planar doubly pyrazolato-bridged copper(II,II) complexes. Taking the difference δ(CuNN) between the deviations of the Cu–N–N and Cu–N′–N′ angles with respect to an optimum angle (130.8°, deduced from the above-mentioned complex with the highest J) as a measure of the asymmetry, a quasi-linearly variation of J with δ(CuNN) was obtained, and indeed the present findings of a large J for a rather symmetric $Cu(NN)_2Cu$ skeleton [Cu–N–N in the range 128.7(4)–130.1(4)°] fits into the proposed model.

Conclusions

A series of potentially dinucleating pyrazolate-based ligands with chelating thioether side arms has been prepared. As a representative example the benzyl derivative **1bH** was employed in the synthesis of the dinuclear Cu^{II} complex **4** displaying distorted square planar N_2S_2 coordination spheres for each copper center and an axially bridging tetrafluoroborate. The magnitude of the antiferromagnetic exchange coupling in **4** ($J = -206$ cm^{-1}) lies in the upper range of the exchange interactions generally found for bis(μ-pyrazolato)-bridged compounds, which is in accord with the structural findings of a rather symmetric framework in the present complex. The electrochemical reduction of **4** is an irreversible two electron process which reflects the inability of the N_2S_2 donor skeleton to conserve the dinuclear array and at the same time adopt a pseudotetrahedral, trigonal or linear geomtry that is preferred by the Cu^I form. Cu^I and Ag^I complexes of **1a**–**1d** were synthesized independently. The crystal structure of the silver complex **3c** reveals the presence of trinuclear species with linear *N*-coordination of the metal centers, where each two of these triangular constituents are linked by two unexpectedly strong unsupported Ag···Ag contacts, i.e. contacts between closed-shell d^{10} systems, resulting in the preservation of hexanuclear entities even in solution. The Cu^I complexes are assumed to adopt analogous structures based on their similar appearance and properties. Consequently the electrochemical oxidation of the Cu^I complexes is an irreversible process, presumably generating a more appropriate coordination environment for Cu^{II}. A possible stabilization of both Cu^{II} and Cu^I in a dinuclear array like in **4** would presumably necessitate more flexible, longer side arms at the pyrazolate to enable the adaptation to pseudotetrahedral coordination of the metal centers upon reduction. Work with respect to this is presently in progress.

We are grateful to Prof. Dr. *G. Huttner* for his generous and continuous support of our work as well as to the *Fonds der Chemischen Industrie* for providing a Liebig-Stipendium (to F. M.). We thank *T. Janack* and Dr. *J. Groß* for recording the MS spectra and *D. Günauer* for performing the cyclovoltammetric measurements.

Experimental Section

All manipulations were carried out under an atmosphere of dry nitrogen by employing standard Schlenk techniques. Solvents were dried according to established procedures. Microanalyses: Mikroanalytische Laboratorien des Organisch-Chemischen Instituts der Universität Heidelberg. – IR spectra: Bruker IFS 66 FTIR. – ^{1}H- and ^{13}C{^{1}H}-NMR spectra: Bruker AC 200 at 200.13 MHz and 50.32 MHz, respectively. Signal of the solvent as chemical shift reference. $CDCl_3$: $\delta_H = 7.27$, $\delta_C = 77.0$; C_6D_6; $\delta_H = 7.15$, $\delta_C = 128.0$. – FAB- and EI-MS spectra: Finnigan MAT 8230; FD-MS spectra: Jeol JMS-700. – UV/Vis/NIR spectra: Perkin-Elmer Lambda 19. – Cyclic voltammetry: PAR equipment (potentiostat/galvanostat 273), in 0.1 M n-Bu_4NPF_6/CH_2Cl_2. Potentials in V on glassy carbon electrode, referenced to saturated calomel electrode (SCE) at ambient temperature. – Magnetic measurements: Bruker Magnet B-E 15 C8, field-controller B-H 15, variable temperature unit ER4111VT, Sartorius micro balance M 25 D-S. – ESR spectra: Bruker ESP 300 E, X-band, external standard DPPH, temperature control unit Eurotherm B-VT 2000. – Vapor-phase osmometry: Knauer Osmometer 7311100000.

Ligands **1aH**–**1dH**: The appropriate thiol (31.0 mmol) is dissolved in thf (80 ml) and deprotonated by means of one equivalent of BuLi (2.5 M in hexane) at 0°C. 3,5-Bis(chloromethyl)pyrazole hydrochloride[10] (10.0 mmol) is then added in one portion and the resulting solution is kept stirring overnight at room temp. After removal of all volatile material under vacuum the residue is taken up in petroleum ether (boiling range 40–60°C) and filtered. Evaporation of the solvent affords the raw product which is purified by column chromatography [40 × 5 cm, silica gel (32–63 μm), ether/petroleum ether (boiling range 40–60°C) (3:1; **1bH**: $R_f = 0.32$; **1cH**: $R_f = 0.27$) (5:1; **1aH**: $R_f = 0.35$; **1dH**: $R_f = 0.40$)] to yield the product as slightly yellowish oil (**1aH**: 2.8 g, 92%; **1bH**: 2.8 g, 82%; **1cH**: 1.9 g, 78%) or white powder (**1dH**: 1.8 g, 66%).

Cu^I and Ag^I Complexes **2a**–**2c** *and* **3a**–**3d**: The appropriate ligand **1aH**–**dH** (1 mmol) is dissolved in thf (25 ml) and deprotonated by slow addition of one equivalent of BuLi (2.5 M in hexane) at –50°C. After warming to room temp. CuCl (0.10 g, 1.0 mmol) or $AgBF_4$ (0.19 g, 1.0 mmol), respectively, is added in one portion and the reaction mixture stirred for 1 h. All volatile material is then removed under vacuum and the residue is taken up in CH_2Cl_2 (30 ml; **2a**, **3a**) or petroleum ether (boiling range 40–60°C; 30 ml; **2b**, **2c**, **3b**–**d**) and filtered. The undissolved inorganic salts are washed twice with CH_2Cl_2 or petroleum ether, respectively, and the combined organic phases are reduced under vacuum to a volume of around 20 ml. Cooling of the resulting solution to –40°C causes precipitation of the product as a white solid, which is isolated by filtration in the cold and dried under vacuum. **2a**: 0.33 g (88%); **2b**: 0.26 g (65%); **2c**: 0.23 g (75%); **3a**: 0.38 g (90%); **3b**: 0.38 g (85%); **3c**: 0.28 g (79%); **3d**: 0.17 g (45%).

Cu^{II} Complex **4**: A solution of **1bH** (0.24 g, 0.7 mmol) in thf (20 ml) is treated dropwise with one equivalent of BuLi (2.5 M in hexane) at –50°C and stirred for 20 min while warming to room temp. Addition of $[Cu(H_2O)_6](BF_4)_2$ (0.24 g, 0.7 mmol) initially yields a green soluton which gradually turns brown and causes precipitation of a dark solid upon stirring for 3 h. Removal of all volatile material under vacuum affords a brown residue which is redissolved in CH_2Cl_2 (20 ml) and filtered. Evaporation of the solvent gives the raw product that can be crystallized by layering a solution in acetone with petroleum ether, yielding 0.27 g (0.26 mmol, 74%) of the solvate **4** · acetone as black crystals. UV/Vis (CH_2Cl_2): λ_{max} (ε) = 480 nm, 330 (9800).

X-ray Structure Determinations: The measurements were carried out on a Siemens P4 (Nicolet Syntex) R3m/v four-circle diffractometer with graphite-monochromated MoK_α radiation. All calculations were performed with a micro-vax computer using the SHELXT PLUS software package. Structures were solved by direct methods with the SHELXS-86 and refined with the SHELX93 programs[36]. An absorption correction (ψ scan, Δψ = 10°) was applied to all data. Atomic coordinates and anisotropic thermal parameters of the non-hydrogen atoms were refined by full-matrix least-squares calculation. For **3c** the isopropyl groups attached to S2 and S6 were disordered and could thus only be refined isotropically. In the case of **4** the fluorine atoms attached to B2 were disordered and refined isotropically, and the large residual electron density (peak and hole) was all located around the disordered BF_4^- ion. Table 7 compiles the data for the structure determinations. Further details of the crystal structure investigations are available from the Fachinformationszentrum Karlsruhe, D-76344 Eggenstein-Leopoldshafen (Germany), on quoting the depository numbers CSD-406568 (**3c**) and 406569 (**4**), the names of the authors, and the journal citation.

Table 7. Crystal data and refinement details for complexes **3c** and **4**

	3c	**4**
Formula	$C_{33}H_{57}Ag_3N_6S_3$	$C_{38}H_{38}B_2Cu_2F_8N_4S_4 \cdot C_3H_6O$
M_r	1053.8	1037.7
crystal size [mm]	0.20 × 0.20 × 0.35	0.30 × 0.30 × 0.40
crystal system	monoclinic	triclinic
space group	$P2_1/n$	$P\bar{1}$
a [Å]	16.037(7)	10.777(3)
b [Å]	11.453(5)	14.393(2)
c [Å]	23.899(8)	14.739(2)
α [°]	90	81.92(1)
β [°]	100.34(3)	79.39(1)
γ [°]	90	87.97(2)
V [Å^3]	4318(3)	2225(1)
$\rho_{calcd.}$ [g cm^{-3}]	1.621	1.549
Z	4	2
$F(000)$ [e]	2136	1060
T [K]	200	200
μ (Mo-K_α) [mm^{-1}]	1.668	1.216
scan mode	ω	ω
hkl range	0–17, 0–12, ±26	0–11, ±15, ±15
2θ range [°]	4.0–47.0	4.1–45.0
measured refl.	6635	6198
Observed refl. $I > 2\sigma(I)$	4415	4148
refined parameters	526	554
resid. electron dens. [eÅ^{-3}]	0.753/–0.484	1.340/–1.999
$R1$	0.045	0.062
$wR2$ (refinement on F^2)	0.081	0.130
Goodness-of-fit	1.021	1.416

---

* Dedicated to Prof. Dr. *Gottfried Huttner* on the occasion of his 60th birthday.

[1] W. Kaim, J. Rall, *Angew. Chem.* **1996**, *108*, 47–64; *Angew. Chem. Int. Ed. Engl.* **1996**, *35*, 43–60; K. D. Karlin, *Bioinorganic Chemistry of Copper*, Chapman & Hall, New York, **1993**. A. G. Sykes, *Adv. Inorg. Chem.* **1991**, *36*, 377–408.

[2] N. Kitajima, *Adv. Inorg. Chem.* **1992**, *39*, 1–77.

[3] E. Bouwman, W. L. Driessen, J. Reedijk, *Coord. Chem. Rev.* **1990**, *104*, 143–171.

[4] [4a] K. C. Tran, J. P. Battioni, J. L. Zimmermann, C. Bois, G. J. A. A. Koolhaas, P. Leduc, E. Mulliez, H. Boumchita, J. Reedijk, J. C. Chottard, *Inorg. Chem.* **1994**, *33*, 2808–2814. – [4b] R. Bentfeld, N. Ehlers, R. Mattes, *Chem. Ber.* **1995**, *128*, 1199–1205.

[5] J. A. Farrar, F. Neese, P. Lappalainen, P. M. H. Kroneck, M. Saraste, W. G. Zumft, A. J. Thomson, *J. Am. Chem. Soc.* **1996**, *118*, 11501–11514.

[6] S. Iwata, C. Ostermeier, B. Ludwig, H. Michel, *Nature* **1995**, *376*, 660–669; T. Tsukihara, H. Aoyama, E. Yamashita, T. Tomizaki, H. Yamaguchi, K. Shinzawa-Itoh, R. Nakashima, R. Yaono, S. Yoshikawa, *Science* **1995**, *269*, 1069–1074; W. E. Antholine, D. H. W. Kastrau, G. C. M. Steffens, G. Buse, W. G. Zumft, P. M. H. Kroneck, *Eur. J. Biochem.* **1992**, *209*, 875–881.

[7] R. P. Houser, J. A. Halfen, V. G. Young, Jr., N. J. Blackburn, W. B. Tolman, *J. Am. Chem. Soc.* **1995**, *117*, 10745–10746; R. P. Houser, V. G. Young, Jr., W. B. Tolman, *J. Am. Chem. Soc.* **1996**, *118*, 2101–2102.

[8] A. F. Stange, E. Waldhör, M. Moscherosch, W. Kaim, *Z. Naturforsch. B* **1995**, *50*, 115–118; N. D. J. Branscombe, A. J. Blake, A. Marin-Becerra, W.-S. Li, S. Parsons, L. Ruiz-Ramirez, M. Schröder, *J. Chem. Soc., Chem. Commun.* **1996**, 2573–2574.

[9] P. J. Steel, *Coord. Chem. Rev.* **1990**, *106*, 227–265; A. P. Sadimenko, S. S. Basson, *ibid.* **1996**, *147*, 247–297.

[10] T. G. Schenck, J. M. Downes, C. R. C. Milne, P. B. Mackenzie, H. Boucher, J. Whelan, B. Bosnich, *Inorg. Chem.* **1985**, *24*, 2334–2337.

[11] [11a] T. Kamiusuki, H. Okawa, N. Matsumoto, S. Kida, *J. Chem. Soc., Dalton Trans.* **1990**, 195–198. – [11b] T. Kamiusuki, H. Okawa, K. Inoue, N. Matsumoto, M. Kodera, S. Kida, *J. Coord. Chem.* **1991**, *23*, 201–211. – [11c] M. Itoh, K. Motoda, K. Shindo, T. Kamiusuki, H. Sakiyama, N. Matsumoto, H. Okawa, *J. Chem. Soc., Dalton Trans.* **1995**, 3635–3641.

[12] B. Mernari, F. Abraham, M. Lagrenee, M. Drillon, P. Legoll, *J. Chem. Soc., Dalton Trans.* **1993**, 1707–1711.

[13] L. Behle, M. Neuburger, M. Zehnder, T. A. Kaden, *Helv. Chim. Acta* **1995**, *78*, 693–702.

[14] F. Meyer, S. Beyreuther, K. Heinze, L. Zsolnai, *Chem. Ber./Recueil* **1997**, *130*, 605–613.

[15] S. Knapp, T. P. Keenan, J. Liu, J. A. Potenza, H. J. Schugar, *Inorg. Chem.* **1990**, *29*, 2189–2191; W. G. Haanstra, M. F. Cabral, J. de O. Cabral, W. L. Driessen, J. Reedijk, *Inorg. Chem.* **1992**, *31*, 3150–3151; R. Prins, M. Biagini-Cingi, M. Drillon, R. A. G. de Graaff, J. Haasnot, A.-M. Manotti-Lanfredi, P. Rabu, J. Reedijk, F. Ugozzoli, *Inorg. Chim. Acta* **1996**, *248*, 35–44.

[16] M. Munakata, L. P. Wu, M. Yamamoto, T. Kuroda-Sowa, M. Maekawa, S. Kawata, S. Kitagawa, *J. Chem. Soc., Dalton Trans.* **1995**, 4099–4106.

[17] R. G. Raptis, J. P. Fackler, Jr., *Inorg. Chem.* **1988**, *27*, 4179–4182.

[18] M. K. Ehlert, S. J. Rettig, A. Storr, R. C. Thompson, J. Trotter, *Can. J. Chem.* **1990**, *68*, 1444–1449; M. K. Ehlert, S. J. Rettig, A. Storr, R. C. Thompson, J. Trotter, *Can. J. Chem.* **1992**, *70*, 2161–2173.

[19] G. A. Ardizzoia, S. Cenini, G. La Monica, N. Masciocchi, M. Moret, *Inorg. Chem.* **1994**, *33*, 1458–1463.

[20] H. Okkersen, W. L. Groeneveld, J. Reedijk, *Recl. Trav. Chim. Pays-Bas* **1973**, *92*, 945–951.

[21] A. Zecchina, L. Cerruti, S. Coluccia, E. Borello, *J. Chem. Soc. (B)* **1967**, 1363–1368.

[22] H. H. Murray, R. G. Raptis, J. P. Fackler, Jr., *Inorg. Chem.* **1988**, *27*, 26–33.

[23] J. F. Modder, J.-M. Ernsting, K. Vrieze, M. de Wit, C. H. Stam, G. van Koten, *Inorg. Chem.* **1991**, *30*, 1208–1214; G. C. van Stein, G. van Koten, K. Vrieze, A. L. Spek, E. A. Klop, C. Brevard, *Inorg. Chem.* **1985**, *24*, 1367–1375; J. F. Modder, K. Vrieze, A. L. Spek, G. Challa, G. van Koten, *Inorg. Chem.* **1992**, *31*, 1238–1247; J. F. Modder, R. J. Leijen, K. Vrieze, W. J. J. Smets, A. L. Spek, G. van Koten, *J. Chem. Soc., Dalton Trans.* **1995**, 4021–4028.

[24] M. Konrad, F. Meyer, M. Büchner, K. Heinze, L. Zsolnai, *Chem. Ber./Recueil* **1997**, *130*, 95–100.

[25] M. J. Schilstra, P. J. M. W. L. Birker, G. C. Verschoor, J. Reedijk, *Inorg. Chem.* **1982**, *21*, 2637–2644.

[26] J. Huheey, E. Keiter, R. Keiter, *Anorganische Chemie*, 2nd ed., Walter de Gruyter, Berlin, **1995**, p. 335.

[27] A. J. Amoroso, J. C. Jeffery, P. L. Jones, J. A. McCleverty, E. Psillakis, M. D. Ward, *J. Chem. Soc., Chem. Commun.* **1995**, 1175–1176; F. Robinson, M. J. Zaworotko, *J. Chem. Soc., Chem. Commun.* **1995**, 2413–2414.

[28] N. Masciocchi, M. Moret, P. Cairati, A. Sironi, A. A. Ardizzoia, G. La Monica, *J. Am. Chem. Soc.* **1994**, *116*, 7668–7676.

[29] D. E. Nikles, M. J. Powers, F. L. Urbach, *Inorg. Chim. Acta* **1979**, *37*, L499–L501; E. I. Solomon, K. W. Penfield, D. E. Wilcox, *Structure and Bonding*, **1983**, *53*, 1–57.

[30] See for example: J. Foley, D. Kennefick, D. Phelan, S. Tyagi, B. Hathaway, *J. Chem. Soc., Dalton Trans.* **1983**, 2333–2338; O. J. Gelling, F. van Bolhuis, A. Meetsma, B. L. Feringa, *J. Chem. Soc., Chem. Commun.* **1988**, 552–554; C. F. Martens, A. P. H. J. Schenning, M. C. Feiters, J. Heck, G. Beurskens, P. T. Beurskens, E. Steinwender, R. J. M. Nolte, *Inorg. Chem.* **1993**, *32*, 3029–3033.

[31] V. P. Hanot, T. D. Robert, J. Kolnaar, J. G. Haasnoot, J. Reedijk, H. Kooijman, A. L. Spek, *J. Chem. Soc., Dalton Trans.* **1996**, 4275–4281.

[32] D. F. Evans, *J. Chem. Soc.* **1959**, 2003–2007.

[33] B. Bleaney, K. D. Bowers, *Proc. R. Soc. (London), Ser. A* **1952**, *214*, 451.

[34] J. Pons, X. Lopez, J. Casabo, F. Teixidor, A. Caubet, J. Rius, C. Miravitlles, *Inorg. Chim. Acta* **1992**, *195*, 61–66.

[35] D. Ajo, A. Bencini, F. Mani, *Inorg. Chem.* **1988**, *27*, 2437–2444.

[36] G. M. Sheldrick, *SHELX93, Program for Crystal Structure Refinement*, Universität Göttingen, **1993**; G. M. Sheldrick, *SHELXS-86, Program for Crystal Structure Solution*, Universität Göttingen, **1986**.

[97042]